

Examining Physiologically-Based Pharmacokinetic (PBPK) Model Assumptions for Cross-Tissue Similarity of k_{cat} : The Case Example of Uridine 5'-diphosphate Glucuronosyltransferase (UGT)

Anika N. Ahmed, Amin Rostami-Hodjegan, Jill Barber, Zubida M. Al-Majdoub

Centre for Applied Pharmacokinetic Research, School of Health Sciences, University of Manchester, UK (A.A., A. R.-H., J.B., Z.M.A); Certara, Simcyp Division, 1 Concourse Way, Sheffield, UK (A. R.-H.)

This work received no external funding

No author has an actual or perceived conflict of interest with the contents of this article

Running title: K_{cat} assessment of UGT enzymes across different organs

Keywords: PBPK, IVIVE, Renal Drug Metabolism, Intestinal Drug Metabolism, k_{cat}

Corresponding author: Dr. Zubida Al-Majdoub; Centre for Applied Pharmacokinetic Research, University of Manchester, Room 3.32, Stopford Building, Oxford road, Manchester, M13 9PT, UK; email: zubida.al-majdoub@manchester.ac.uk

Type: Commentary (Invited)

Number of text pages: 21

Number of Tables: 5

Number of Figures: 2

Number of References: 41

Number of words in Abstract: 230

Number of words in Introduction: 562

Number of words in Discussion: 1,367

Abbreviations

UGT, Uridine 5'-diphosphate glucuronosyltransferase; CYP, cytochrome P450; DDIs, drug-drug interactions; IVIVE, *in vitro-in vivo* extrapolation; PBPK, physiologically-based pharmacokinetics; $CL_{int,u}$, unbound intrinsic clearance

Abstract

The default assumption during *in vitro in vivo* extrapolation (IVIVE) to predict metabolic clearance in physiologically-based pharmacokinetics (PBPK) is that protein expression and activity have the same relationship in various tissues. This assumption is examined for uridine 5'-diphosphate glucuronosyltransferases (UGTs), a case example where expression and, hence, metabolic activity are distributed across various tissues. Our literature analysis presents overwhelming evidence of a greater UGT activity per unit of enzyme (higher k_{cat}) in kidney and intestinal tissues relative to liver (greater than 200-fold for UGT2B7). This analysis is based on application of abundance values reported using similar proteomic techniques and within the same laboratory. Our findings call into question the practice of assuming similar k_{cat} during IVIVE estimations as part of PBPK, and call for a systematic assessment of the k_{cat} of various enzymes across different organs. The analysis focused on compiling data for probe substrates that were common for two or more of the studied tissues, to allow for reliable comparison of cross-tissue enzyme kinetics; this meant that UGT enzymes included in the study were limited to UGT1A1, 1A3, 1A6, 1A9 and 2B7. Significantly, UGT1A9 (n=24) and the liver (n=27) were each found to account for around half of the total dataset; these were found to correlate, with hepatic UGT1A9 data found in 15 of the studies, highlighting the need for more research into extrahepatic tissues and other UGT isoforms.

SIGNIFICANCE STATEMENT

During PBPK modelling (*in vitro in vivo* extrapolation) of drug clearance, the default assumption is that the activity per unit of enzyme (k_{cat}) is the same in all tissues. The analysis provides preliminary evidence that this may not be the case, and that renal and intestinal tissues may have almost 250-fold greater UGT activity per unit of enzyme than liver tissues.

Introduction

Applications of physiologically-based pharmacokinetics (PBPK) over the last 20 years have increased exponentially compared with the rest of pharmacokinetics (El-Khateeb *et al.*, 2021). This has been linked to the ability of PBPK models to extrapolate kinetics beyond the average patient by using fundamental aspects of the biology related to the change of the expression in enzymes between healthy individuals and various patient groups (Howard *et al.*, 2018).

The default assumption during the *in vitro in vivo* extrapolation (IVIVE) steps of metabolic information for drug clearance during PBPK is that expression mirrors activity regardless of the location of the enzyme. In other words, the activity per unit of enzyme (so called k_{cat}) is considered to be the same in various tissues. We wished to examine this common assumption for the case example of uridine 5'-diphosphate glucuronosyltransferase (UGT) enzymes. These enzymes are involved in phase II biotransformation of many drugs, and they are currently the second most common route for primary drug metabolism, responsible for the metabolic clearance of 10-30% of all drugs (Stingl *et al.*, 2014). This proportion is set to increase, as pharmaceutical companies are intentionally designing new drug candidates that go through non-cytochrome P450 (CYP) pathways, in order to reduce the burden of CYP-related drug-drug interactions (DDIs) (Achour *et al.*, 2014).

Previous research has identified the liver as the epicentre of xenobiotic metabolic processes, containing the most diverse and abundant population of drug metabolising enzymes (Achour *et al.*, 2014). However, some may argue that the contributions of other key metabolic tissues involved in drug disposition have been neglected or under-estimated. Studies involving extrahepatic metabolism are very limited compared with hepatic metabolism (Scotcher *et al.*, 2016), and in order to build a clinically realistic model of the human body, the involvement of enzyme kinetics across extrahepatic tissues must be quantified. This is as true of UGTs as of other enzymes. UGT enzymes quantified in the liver do not have a complete set of corresponding expression values in renal and intestinal tissues (Achour *et al.*, 2014; Al-Majdoub *et al.*, 2021; Couto *et al.*, 2020). This highlights the need to generate a reliable dataset for absolute enzyme abundances across the key metabolic organs, as a starting point for quantifying tissue-specific enzyme kinetics.

In order to begin quantifying UGT enzyme kinetics per unit of enzyme, absolute abundance for individual UGT isoforms must be determined, as amount of enzyme per milligram of microsomal protein (Crewe *et al.*, 2011). V_{\max} , measurable as amount of isoform-specific probe substrate converted to its metabolite per unit time, must also be determined. The enzyme abundance-activity relationship can then be quantified as k_{cat} , defining the differences in intrinsic activity per unit of UGT. In order to accurately reflect tissue-specific kinetics, k_{cat} must account for tissue-specific enzyme abundances (Robinson, 2015). The common assumption that k_{cat} is the same across various tissues has not been examined for UGTs and information on other enzymes is sparse (Galetin and Houston, 2006; von Richter *et al.*, 2004; Yang *et al.*, 2004).

Obviously, the accuracy of clearance predictions will also depend on correct assignment of the extrahepatic metabolism. However, this is not the subject of current exercise. Nonetheless, we make extensive use of the research into the abundance (Achour *et al.*, 2014) and activity of UGT in intestine and kidney even though abundance values are missing for several UGT enzymes (Couto *et al.*, 2020; Al-Majdoub *et al.*, 2021).

Materials and Methods

Collection of data

Two electronic databases, Web of Science (<https://wok.mimas.ac.uk>) and PubMed (<https://www.ncbi.nlm.nih.gov/pubmed/>) were searched for relevant literature, between the years 2000-2019, using appropriate keywords (UDP-glucuronosyltransferase, UGT activity). Both UGT abundance and activity studies were searched for glucuronidation data; this involved searching for other key terms in place of ‘activity’ to widen the search scope (glucuronidation, k_{cat} , metabolism, abundance, concentration, content, quantification, measurement, LC-MS, ELISA, Western blotting). Citation lists within the collected studies were also inspected to identify any further relevant literature. Searches were species and tissue-specific for human intestinal and kidney microsomes; keywords included synonyms for these tissues (gut, renal). The search criteria were repeated for human liver microsomes, focusing on literature using the probe substrates identified in renal and intestinal studies, to compile a database of comparable data. All but one publication included data from ‘adult’ populations; hence only data generated from adult tissue samples were included for analysis.

Calculation of enzyme activity

The k_{cat} values for individual UGT isoforms were calculated using equation 1, where V_{max} represents the maximal metabolic capacity in pmol/min/mg microsomal protein, and UGT abundance is tissue-specific for individual isoforms in pmol UGT/mg protein.

$$k_{cat} \text{ (pmol/min/pmol UGT)} = V_{max} \text{ (pmol/min/mg protein)} / \text{Abundance UGT (pmol UGT/mg protein)} \dots \dots \dots (1)$$

Where V_{max} was not specified for activity, K_m values (substrate concentration at $\frac{1}{2}V_{max}$) were identified for the probe substrates; if the probe concentration (μM) was found to be significantly above the maximum K_m value (μM), i.e., >2-fold, the assumption was made that the reaction was conducted at V_{max} , and these data were used to calculate k_{cat} . On the other hand, if the probe concentration (μM) was found to be significantly below the minimum K_m value (μM), i.e., <0.5-fold, the assumption was made that the activity value was within the intrinsic clearance range and the clearance was used as a supplementary measurement of enzyme activity. Here, the literature was examined to identify reported probe K_m values; and where this information was not available, reference K_m values were found (Miners *et al.*, 2021; Seo *et al.*, 2016). We have to acknowledge that our assumption will result in significant errors in the calculation of these parameters, depending on how far the substrate concentrations deviate from those related to initial rate (in which case $CL_{int, UGT} = V_{max}/(K_m)$ and V_{max} . However, the error introduced by this approach will be less than that associated with the comparison of kinetic data from studies that utilized vastly different experimental conditions. Where necessary, intrinsic clearance data were corrected for the microsomal fraction of unbound drug, to give $CL_{int,u}$, a closer estimate for *in vivo* clearance (Gao *et al.*, 2008; Hallifax and Houston, 2006). Once the corrected clearance values had been determined, $CL_{int,u}$ ($\mu\text{L}/\text{min}/\text{mg}$ microsomal protein) values were divided by the abundance (pmol/mg protein) and probe concentrations (μM) to give $CL_{int,u}$ per unit enzyme ($\mu\text{L}/\text{min}/\text{pmol}$ enzyme).

Results

Filtering data

A total of 19 studies were used in this analysis; 15 of these were relevant for calculating k_{cat} (Achour *et al.*, 2018; Al-Jahdari *et al.*, 2006; Benoit-Biancamano *et al.*, 2008; Chen *et al.*, 2018;

Gill *et al.*, 2013; Knights *et al.*, 2016; Komura and Iwaki, 2011; Liang *et al.*, 2011; Miles *et al.*, 2005; Picard *et al.*, 2005; Rowland *et al.*, 2008; Shimizu *et al.*, 2007; Soars *et al.*, 2001; Soars *et al.*, 2003; Walsky *et al.*, 2012), whilst the remaining four were used for calculating $CL_{int,u}$ (Bhatt *et al.*, 2019; Cubitt *et al.*, 2009; Gill *et al.*, 2012; Scotcher *et al.*, 2017). Of the total dataset, 29% of the data did not meet the search criteria and were excluded, on account of: no probe specificity, no availability of abundance data, or did not fall into the V_{max} or intrinsic clearance range. The data useful in this analysis are summarized in Table 1. Probes were selected based on availability of data across two or (preferably) all of the studied tissues; because data were very limited, it was necessary to focus on availability rather than specificity of probes. Data were available for UGT1A1, 1A6, 1A9 and 2B7 for k_{cat} calculations. Only UGT1A6, with probe substrate deferiprone, was comparable across all three tissues (Benoit-Biancamano *et al.*, 2009; Knights *et al.*, 2016); UGT1A1 was comparable across the liver and intestine (Komura and Iwaki, 2011), whilst data for UGT1A9 and 2B7 were comparable across the liver and kidney (Knights *et al.*, 2016; Komura and Iwaki, 2011; Miles *et al.*, 2005). Intrinsic clearance calculations allowed for comparison of UGT1A1 and 1A3 across all three tissues, using probe substrates ezetimibe and telmisartan, respectively (Gill *et al.*, 2012); UGT1A9 data was comparable across the liver and kidneys (Bhatt *et al.*, 2019; Gill *et al.*, 2012; Scotcher, *et al.*, 2017), whilst data for UGT2B7 was comparable across the liver and intestine (Gill *et al.*, 2012).

Reference abundance values

The collated reference abundance values (Achour *et al.*, 2014; Al-Majdoub *et al.*, 2021; Couto *et al.*, 2020), presented in Table 2, were used to perform k_{cat} and $CL_{int,u}$ calculations, where activity data did not have corresponding abundance values presented in the literature (Al-Jahdari *et al.*, 2006; Benoit-Biancamano *et al.*, 2008; Chen *et al.*, 2018; Cubitt *et al.*, 2009; Gill *et al.*, 2012; Gill *et al.*, 2013; Komura and Iwaki, 2011; Liang *et al.*, 2011; Miles *et al.*, 2005; Picard *et al.*, 2005; Rowland *et al.*, 2008; Scotcher *et al.*, 2017; Shimizu *et al.*, 2007; Soars *et al.*, 2001; Soars *et al.*, 2003; Walsky *et al.*, 2012).

UGT isoforms included in the analysis were based on availability of common probes and activity data (at V_{max}) across two or more of the tissues (UGT1A1, 1A3, 1A6, 1A9 and 2B7); however, a

wider range of enzyme expressions are demonstrated in Table 2, in order to highlight data availability across tissues.

Correlation of UGT expression and activity between different tissues

The reported activity values for human liver, intestine and kidney microsomes, used to calculate k_{cat} and $CL_{int,u}$, are demonstrated in Tables 3 and 4, respectively. Some assumptions for V_{max} were made for data used for calculating mean k_{cat} (Table 3), where V_{max} was not specified but probe concentration was found to be more than 2-fold greater than the substrate K_m (Knights et al., 2016). Similarly, for $CL_{int,u}$ calculations, where activity data were not specified as V_{max} , it was assumed to be in the intrinsic clearance range, if probe concentration was found to be less than 0.5-fold of the substrate concentration (Bhatt *et al.*, 2019). Where activity was assumed to be at V_{max} or intrinsic clearance, probe substrate concentration and K_m have also been recorded. Probe concentration was recorded across all $CL_{int,u}$ enzymes, in order to calculate $CL_{int,u}$ per unit enzyme (see ‘*Methods and Materials*’). Key experimental differences, which may have influenced on the activities seen across the studies, are recorded in Table 5.

In order to demonstrate the differences in the mean relative expressions and activities of UGT enzymes across the tissues, scatter graphs were generated, with the y-axis in logarithmic scale (\log_{10}), demonstrating the ratio of fold difference of intestinal and renal abundances and activities, relative to the liver (Figures 1, 2). Data for enzyme activities were segregated for k_{cat} and $CL_{int,u}$ (Figure 2A, B). The reference line for the liver crosses the y-axis horizontally at 1; values above or below the line represent greater or fewer enzyme expression, respectively, found in the intestine and kidneys than that found in the liver.

Discussion

This analysis uniquely reviews a comprehensive list of all significant UGT activity studies conducted using comparable probe substrates for human liver, intestinal and kidney microsomal tissues, between 2000-2019. Nevertheless, it only provides a preliminary database of mean activity values, as k_{cat} and $CL_{int,u}$, for comparable UGT isoforms for the three major metabolic organs since the functional assays were not conducted in the same laboratory nor under exactly similar conditions. We were able to map a ratio of fold difference for the intestine and kidney relative to

liver for UGT enzyme abundance, but more importantly activity per unit of enzyme. The intestinal and kidney abundance data, which we used for calculating activity per unit of enzyme, were all taken from a single laboratory (i.e., the University of Manchester, Table 2). Achour *et al.*'s 2014 meta-analysis presented weighted average abundance values for liver from data published between 1980-2014 measured using LC-MS proteomics and was used for calculating k_{cat} values in liver (Achour *et al.*, 2014). Mean renal and intestinal (from kidney cortex) abundance data were taken from recent studies (Al-Majdoub *et al.*, 2021; Couto *et al.*, 2020), respectively, using the same laboratory environments, LC-MS technology and consistent assay conditions. Consistency in LC-MS-based quantification across the three studies, with abundance reported in the microsomal fraction (pmol/mg microsomal protein), provides a reliable source of reference abundance values. This degree of consistency in abundance values, used for the calculation of cross-tissue enzyme kinetics, has not been accomplished in any other UGT activity study; it also provides a reference point for cross-tissue UGT enzyme expressions for future research.

Our major objective in this analysis was to explore the assumption of similarity in k_{cat} , for UGT enzymes across the liver, intestine and kidneys, as a case example. Because there is limited research into UGT functional assays involving full kinetics (at different concentrations), we could not calculate k_{cat} in many cases and used $CL_{int,u}$ per unit enzyme instead (measured at low concentrations of the probe). We focused on data for probes that were common for functional assays conducted at least in two of the tissues. Accordingly, the analysis was limited to UGT1A1, 1A3, 1A6, 1A9 and 2B7. Among these, UGT1A9 (n=24) and the liver (n=27) comprised almost half of the data for the analysis (Achour *et al.*, 2018; Al-Jahdari *et al.*, 2006; Bhatt *et al.*, 2019; Chen *et al.*, 2018; Gill *et al.*, 2012; Gill *et al.*, 2013; Komura and Iwaki, 2011; Liang *et al.*, 2011; Miles *et al.*, 2005; Picard *et al.*, 2005; Rowland *et al.*, 2008; Shimizu *et al.*, 2007; Soars *et al.*, 2001; Soars *et al.*, 2003; Walsky *et al.*, 2012), emphasizing the paucity of functional assays conducted in extrahepatic tissues for majority of UGT isoforms.

Although UGT abundances are unsurprisingly greater within the liver across all measured isoforms (Figure 1), activity per unit of enzyme appears to be lower in the liver than in the other tissues. There was an overall trend when UGT functional activities were available across all three tissues (UGT1A6 (k_{cat}), 1A1, 1A3 and 2B7 ($CL_{int,u}$)). These results therefore suggest that the relative contribution of drug metabolism by liver may have been assigned incorrectly for UGT substrates.

This is when PBPK models assume the same metabolic clearance by UGT per unit of enzyme in various tissues. A renal k_{cat} of more than 200-fold greater than the liver (e.g., UGT2B7) can compensate greatly for a 300-fold lower abundance relative to liver (e.g., UGT1A1).

Contribution of any enzyme to overall kinetics also depends on other factors, such as the blood flow to the organ and the topological arrangements related to the physiology and anatomy (Nishimura *et al.*, 2007; Pang *et al.*, 2019). In addition, enzyme-specific cofactors (for example, UDP-glucuronic acid (UDPGA) is a glucuronic donor in glucuronidation reactions) are critical. Lack of UDPGA, which needs to be at least 5 mM for optimum glucuronidation activity, and simplification of kinetic analyses leads to loss of activity in all UGT isoforms. Although specific probe substrates have in fact been identified for UGT enzymes (Miners *et al.*, 2021), the analysis in the current study was limited by the lack of enzyme activity data measured using these specific probe substrates - a common research gap for non-CYP enzymes (Argikar *et al.*, 2016). Hence, the data in this study was limited by the non-specificity of some of the probes used for measuring activity (i.e., ezetimibe and naloxone), as data was selected based on availability of comparable probes across the studied tissues. Nevertheless, most of the isoforms could be assessed with confidence using specific probe data: UGT1A3, 1A6, 1A9 and 2B7, using telmisartan, deferiprone, propofol, mycophenolic acid and zidovudine, respectively (Miners *et al.*, 2021). For the remaining UGT enzymes, there is a clear research gap. For instance, while UGT1A9 activity values were available for hepatic, intestinal and renal tissues as both V_{max} and $CL_{int,u}$, there was a lack of intestinal abundance data, and k_{cat} and $CL_{int,u}$ (per unit enzyme) could not be calculated across all organs (Gill *et al.*, 2012; Gill *et al.*, 2013; Komura and Iwaki, 2011; Picard *et al.*, 2005; Shimizu *et al.*, 2007).

Consistency between the protocols measuring the functional activity is another issue that hampers the robust assessment of the k_{cat} across the tissues based on literature data (Table 5). The requirement for a minimum concentration of UDPGA of 5mM (Miners *et al.*, 2021) was met in only half the studies (Achour *et al.*, 2018; Cubitt *et al.*, 2009; Gill *et al.*, 2012; Gill *et al.*, 2013; Liang *et al.*, 2011; Rowland *et al.*, 2008; Scotcher *et al.*, 2017; Soars *et al.*, 2001; Soars *et al.*, 2003; Walskey *et al.*, 2012). Factors known to affect V_{max} include: the concentration of alamethicin in the incubation buffer and the time of preincubation of human tissue microsomes with alamethicin, concentration of magnesium chloride ($MgCl_2$), and choice of organic solvent used for

aglycone solubilization in the incubation medium (Miners *et al.*, 2021). Thus, differences in these assay conditions across the studies (Table 5), were expected to have an impact on calculated k_{cat} (Table 3). Bovine serum albumin (BSA) binds free fatty acids which inhibit UGT activity, and is therefore frequently included as a component of incubation buffers. Its presence usually results in an increase in measured intrinsic clearance (fraction unbound) for UGT1A9 and UGT2B7 substrates, as a result of reduction in the K_m (Wu *et al.*, 2013). However, BSA levels were inconsistent across the protocols for assessing functional activity of UGT (Table 5), which may have reduced accuracy in calculated $CL_{int,u}$ (Table 4). Badée *et al.*, (2019) showed mean $CL_{int,u}$ values are dependent on the nature and concentration of the buffer, with reduced buffer concentration seen to reduce the rate of glucuronidation. Table 5 shows the buffers used in studies cited here. Despite these interlaboratory differences, the trends seen in this analysis are consistent in showing greater glucuronidation activities across the intestine and kidney tissues than the liver (Figure 2A, B).

The abundance measurements suffered much less from these concerns. We were able to use proteomic measurements generated in a single laboratory in this study, so the general lack of interlaboratory consistency in quantifying intestinal and renal UGT enzymes did not apply in the present study (Couto *et al.*, 2020, Al-Majdoub *et al.*, 2021). Moreover, hepatic data taken from Achour *et al.*'s 2014 meta-analysis uses literature measuring abundance with LC-MS proteomic technology, much like the intestinal and renal studies, maintaining consistency in the standards used for measuring abundance. Going forward, it is imperative to develop and utilize standardized experimental conditions for future UGT enzyme kinetic research, in order to generate reliable cross-study comparisons.

In conclusion, this preliminary analysis provides a start-point for building tissue-specific IVIVE data. The methods are generalizable to other enzymes involved in drug metabolism. These are important for continuous improvements to PBPK simulations in the development of new drugs. As this case study for UGTs illustrates, accurate estimates of functional enzyme kinetics in various tissues are still limited. It would be desirable to conduct functional assays on the same samples as proteomic measurements, in order to confirm the preliminary findings presented here. Nevertheless, our results suggest that k_{cat} may vary from tissue to tissue, perhaps even within similar tissues depending upon disease state.

Authorship contributions

Participated in research design: Ahmed, Rostami-Hodjegan, Al-Majdoub

Literature search: Ahmed, Al-Majdoub

Performed data analysis: Ahmed

Wrote or contributed to the writing of the manuscript: Ahmed, Rostami-Hodjegan, Barber, Al-Majdoub

References

- Achour B, Dantonio A, Niosi M, Novak JJ, Al-Majdoub ZM, Goosen TC, Rostami-Hodjegan A, and Barber J (2018) Data Generated by Quantitative Liquid Chromatography-Mass Spectrometry Proteomics Are Only the Start and Not the Endpoint: Optimization of Quantitative Concatemer-Based Measurement of Hepatic Uridine-5'-Diphosphate–Glucuronosyltransferase Enzymes with Ref. *Drug Metab Dispos* **46**: 805–812.
- Achour B, Dantonio A, Niosi M, Novak JJ, Fallon JK, Barber J, Smith PC, Rostami-Hodjegan A, and Goosen TC (2017) Quantitative characterization of major hepatic UDP-glucuronosyltransferase enzymes in human liver microsomes: Comparison of two proteomic methods and correlation with catalytic activity. *Drug Metab Dispos* **45**: 1102–1112.
- Achour B, Rostami-Hodjegan A, and Barber J (2014) Protein expression of various hepatic uridine 5'-diphosphate glucuronosyltransferase (UGT) enzymes and their inter-correlations: a meta-analysis. *Biopharm Drug Dispos* **35**: 353–361.
- Al-Jahdari WS, Yamamoto K, Hiraoka H, Nakamura K, Goto F, and Horiuchi R (2006) Prediction of total propofol clearance based on enzyme activities in microsomes from human kidney and liver. *Eur J Clin Pharmacol* **62**: 527–533.
- Al-Majdoub ZM, Scotcher D, Achour B, Barber J, Galetin A, and Rostami-Hodjegan A (2021) Quantitative Proteomic Map of Enzymes and Transporters in the Human Kidney: Stepping Closer to Mechanistic Kidney Models to Define Local Kinetics. *Clin Pharmacol Ther* **110**: 1389-1400.
- Argikar UA, Potter PM, Hutzler JM, and Marathe PH (2016) Challenges and Opportunities with Non-CYP Enzymes Aldehyde Oxidase, Carboxylesterase, and UDP-Glucuronosyltransferase: Focus on Reaction Phenotyping and Prediction of Human Clearance. *AAPS J* **18**: 1391–1405.
- Badée J, Qiu N, Parrott N, Collier AC, Schmidt S, Fowler S (2019) Optimization of Experimental Conditions of Automated Glucuronidation Assays in Human Liver Microsomes Using a Cocktail Approach and Ultra-High Performance Liquid Chromatography–Tandem Mass Spectrometry. *Drug Metab Dispos* **47**: 124-134.
- Benoit-Biancamano MO, Connelly J, Villeneuve L, Caron P, and Guillemette C (2009) Deferiprone glucuronidation by human tissues and recombinant UDP

- glucuronosyltransferase 1A6: An in vitro investigation of genetic and splice variants. *Drug Metab Dispos* **37**: 322–329.
- Bhatt DK, Mehrotra A, Gaedigk A, Chapa R, Basit A, Zhang H, Choudhari P, Boberg M, Pearce RE, Gaedigk R, Broeckel U, Leeder JS, and Prasad B (2019) Age- and Genotype-Dependent Variability in the Protein Abundance and Activity of Six Major Uridine Diphosphate-Glucuronosyltransferases in Human Liver. *Clin Pharmacol Ther* **105**: 131–141.
- Chen A, Zhou X, Cheng Y, Tang S, Liu M, and Wang X (2018) Design and optimization of the cocktail assay for rapid assessment of the activity of UGT enzymes in human and rat liver microsomes. *Toxicol Lett* **295**: 379–389.
- Couto N, Al-Majdoub ZM, Gibson S, Davies PJ, Achour B, Harwood MD, Carlson G, Barber J, Rostami-Hodjegan A, and Warhurst G (2020) Quantitative Proteomics of Clinically Relevant Drug-Metabolizing Enzymes and Drug Transporters and Their Intercorrelations in the Human Small Intestine. *Drug Metab Dispos* **48**: 245–254.
- Crewe HK, Barter ZE, Rowland Yeo K, and Rostami-Hodjegan A (2011) Are there differences in the catalytic activity per unit enzyme of recombinantly expressed and human liver microsomal cytochrome P450 2C9? A systematic investigation into inter-system extrapolation factors. *Biopharm Drug Dispos* **32**: 303–318.
- Cubitt HE, Houston JB, and Galetin A (2009) Relative Importance of Intestinal and Hepatic Glucuronidation—Impact on the Prediction of Drug Clearance. *Pharm Res* **26**: 1073–1083.
- El-Khateeb E, Burkhill S, Murby S, Amirat H, Rostami-Hodjegan A, and Ahmad A (2021) Physiological-based pharmacokinetic modeling trends in pharmaceutical drug development over the last 20-years; in-depth analysis of applications, organizations, and platforms. *Biopharm Drug Dispos* **42**: 107-117.
- Galetin A, and Houston JB (2006) Intestinal and hepatic metabolic activity of five cytochrome P450 enzymes: Impact on prediction of first-pass metabolism. *J Pharmacol Exp Ther* **318**: 1220–1229.
- Gao H, Yao L, Mathieu HW, Zhang Y, Maurer TS, Troutman MD, Scott DO, Ruggeri RB, and Lin J (2008) In silico modeling of nonspecific binding to human liver microsomes. *Drug Metab Dispos* **36**: 2130–2135.

- Gill KL, Gertz M, Houston JB, and Galetin A (2013) Application of a Physiologically Based Pharmacokinetic Model to Assess Propofol Hepatic and Renal Glucuronidation in Isolation: Utility of In Vitro and In Vivo Data. *Drug Metab Dispos* **41**: 744–753.
- Gill KL, Houston JB, and Galetin A (2012) Characterization of in vitro glucuronidation clearance of a range of drugs in human kidney microsomes: Comparison with liver and intestinal glucuronidation and impact of albumin. *Drug Metab Dispos* **40**: 825–835.
- Hallifax D, and Houston JB (2006) Binding of Drugs To Hepatic Microsomes: Comment and Assessment of Current Prediction Methodology with Recommendation for Improvement: Fig. 1. *Drug Metab Dispos* **34**: 724–726.
- Howard M, Barber J, Alizai N, and Rostami-Hodjegan A (2018) Dose adjustment in orphan disease populations: the quest to fulfill the requirements of physiologically based pharmacokinetics. *Expert Opin Drug Metab Toxicol* **14**: 1315–1330.
- Knights KM, Spencer SM, Fallon JK, Chau N, Smith PC, and Miners JO (2016) Scaling factors for the in vitro - in vivo extrapolation (IV-IVE) of renal drug and xenobiotic glucuronidation clearance. *Br J Clin Pharmacol* **81**: 1153–1164.
- Komura H, and Iwaki M (2011) In vitro and in vivo small intestinal metabolism of CYP3A and UGT substrates in preclinical animals species and humans: species differences. *Drug Metab Rev* **43**: 476–498.
- Liang S-C, Ge G-B, Liu H-X, Shang H-T, Wei H, Fang Z-Z, Zhu L-L, Mao Y-X, and Yang L (2011) Determination of propofol UDP-glucuronosyltransferase (UGT) activities in hepatic microsomes from different species by UFLC–ESI-MS. *J Pharm Biomed Anal* **54**: 236–241.
- Miles KK, Stern ST, Smith PC, Kessler FK, Ali S, and Ritter JK (2005) An investigation of human and rat liver microsomal mycophenolic acid glucuronidation: Evidence for a principal role of UGT1A enzymes and species differences in UGT1A specificity. *Drug Metab Dispos* **33**: 1513–1520.
- Miners J, Rowland A, Novak J, Lapham K, Goosen T (2021). Evidence-based strategies for the characterisation of human drug and chemical glucuronidation in vitro and UDP-glucuronosyltransferase reaction phenotyping. *Pharmacol Ther* **218**: 107689.
- Nishimura T, Amano N, Kubo Y, Ono M, Kato Y, Fujita H, Kimura Y, and Tsuji A (2007) Asymmetric intestinal first-pass metabolism causes minimal oral bioavailability of midazolam in cynomolgus monkey. *Drug Metab Dispos* **35**:1275–1284.

- Pang KS, Han YR, Noh K, Lee PI, and Rowland M (2019) Hepatic clearance concepts and misconceptions: Why the well-stirred model is still used even though it is not physiologic reality? *In Biochem. Pharmacol* (Vol. 169), Elsevier Inc.
- Picard N, Ratanasavanh D, Prémaud A, le Meur Y, and Marquet P (2005) Identification of the UDP-glucuronosyltransferase isoforms involved in mycophenolic acid phase II metabolism. *Drug Metab Dispos* **33**: 139–146.
- Robinson PK (2015) Enzymes: principles and biotechnological applications. *Essays Biochem* **59**: 1–41.
- Rowland A, Knights KM, Mackenzie PI, and Miners JO (2008) The “Albumin Effect” and Drug Glucuronidation: Bovine Serum Albumin and Fatty Acid-Free Human Serum Albumin Enhance the Glucuronidation of UDP-Glucuronosyltransferase (UGT) 1A9 Substrates but Not UGT1A1 and UGT1A6 Activities. *Drug Metab Dispos* **36**: 1056–1062.
- Scotcher D, Billington S, Brown J, Jones CR, Brown CDA, Rostami-Hodjegan A, and Galetin A (2017) Microsomal and Cytosolic Scaling Factors in Dog and Human Kidney Cortex and Application for In Vitro-In Vivo Extrapolation of Renal Metabolic Clearance. *Drug Metab Dispos* **45**: 556–568.
- Scotcher D, Jones C, Posada M, Galetin A, and Rostami-Hodjegan A (2016) Key to Opening Kidney for In Vitro-In Vivo Extrapolation Entrance in Health and Disease: Part II: Mechanistic Models and In Vitro-In Vivo Extrapolation. *AAPS J* **18**: 1082–1094.
- Seo K, Kim H, Jeong ES, Abdalla N, Choi C, Kim D, Shin J (2014) In Vitro Assay of Six UDP-Glucuronosyltransferase Isoforms in Human Liver Microsomes, using Cocktails of Probe Substrates and Liquid Chromatography-Tandem Mass Spectrometry. *Drug Metab Dispos* **42**: 1803-1810.
- Shimizu M, Matsumoto Y, and Yamazaki H (2007) Effects of Propofol Analogs on Glucuronidation of Propofol, an Anesthetic Drug, by Human Liver Microsomes. *Drug Metab Lett* **1**: 77–79.
- Soars MG, Riley RJ, Findlay KAB, Coffey MJ, and Burchell B (2001) Evidence for significant differences in microsomal drug glucuronidation by canine and human liver and kidney. *Drug Metab Dispos* **29**: 121–126.
- Soars MG, Ring BJ, and Wrighton SA (2003) The Effect of Incubation Conditions on the Enzyme Kinetics of UDP-Glucuronosyltransferases. *Drug Metab Dispos* **31**: 762–767.

- Stingl JC, Bartels H, Viviani R, Lehmann ML, and Brockmüller J (2014) Relevance of UDP-glucuronosyltransferase polymorphisms for drug dosing: A quantitative systematic review. *Pharmacol Ther* **141**: 92–116.
- von Richter O, Burk O, Fromm MF, Thon KP, Eichelbaum M, and Kivistö KT (2004) Cytochrome P450 3A4 and P-glycoprotein expression in human small intestinal enterocytes and hepatocytes: A comparative analysis in paired tissue specimens. *Clin Pharmacol Ther* **75**: 172–183.
- Walsky RL, Bauman JN, Bourcier K, Giddens G, Lapham K, Negahban A, Ryder TF, Obach RS, Hyland R, and Goosen TC (2012) Optimized assays for human UDP-glucuronosyltransferase (UGT) activities: Altered alamethicin concentration and utility to screen for UGT inhibitors. *Drug Metab Dispos* **40**: 1051–1065.
- Wu B, Dong D, Hu M, and Zhang S (2013) Quantitative Prediction of Glucuronidation in Humans Using the In Vitro- In Vivo Extrapolation Approach. *Cur Top Med Chem* **13**: 1343–1352.
- Yang J, Tucker G, and Rostami-Hodjegan A (2004) Cytochrome P450 3A expression and activity in the human small intestine. *Clin Pharmacol Ther* **76**: 391–391.

Tables

Table 1. Summary of the activity data available for analysis (k_{cat} and $CL_{int,u}$ data combined), with a sum total of data for each probe-specific UGT enzyme, and a sum total of data for each tissue

Enzyme	Probe	Liver	Intestine	Kidney	n = Total data for each enzyme
UGT1A1	Ezetimibe	2	2	1	5
UGT1A3	Telmisartan	1	1	1	3
UGT1A6	Deferiprone	1	1	2	4
UGT1A9	Propofol	12	0	5	17
UGT1A9	MPA*	4	0	3	7
UGT2B7	AZT*	3	0	1	4
UGT2B7	Naloxone	4	2	2	8
Total		27	6	15	48

*MPA, Mycophenolic acid; AZT, Zidovudine

Table 2. Mean abundance values from the literature, for UGT isoforms across human liver, intestine and kidney microsomes (pmol/mg protein)

UGT isoform	1A1*	1A3*	1A4	1A6*	1A9*	2B4	2B7*	2B10	2B15	2B17
Liver ^a	41	31.4	55.4	40	32	57	87	20	52	18
Intestine ^b	1.87	1.14	–	0.75	–	–	1.34	–	0.37	–
Kidney ^c	0.14	0.14	0.2	0.25	2.62	–	1.52	–	–	–

^aAchour *et al.*, 2014; ^bCouto *et al.*, 2020; ^cAl-Majdoub *et al.*, 2021

*Useful for calculating k_{cat} and $CL_{int,u}$ based on availability of data on common probes and activity across two or more of the tissues, identified in the literature

Table 3. V_{max} (pmol/min/mg microsomal protein) and calculated k_{cat} (pmol/min/pmol enzyme) data for UGT enzymes using probe substrates across human liver, intestine and kidney tissues

Enzyme/ identified probe	Probe		Liver		Intestine		Kidney		Study
	Conc. (μ M)	K_m (μ M) ^b	V_{max}	k_{cat}	V_{max}	k_{cat}	V_{max}	k_{cat}	
UGT1A1 <i>Ezetimibe</i>	–	–	4400	107	3020	1610	–	–	Komura and Iwaki, 2011
UGT1A6 <i>Deferiprone</i>	–	–	19300	483	1250	1670	14800	59200	Benoit-Biancamano <i>et al.</i> , 2008 Knights <i>et al.</i> , 2016
	20000	4000 ¹	–	–	–	–	21000	4470	
UGT1A9 <i>Propofol</i>	–	–	2420	65.3	–	–	–	–	Achour <i>et al.</i> , 2018 Al Jahdari <i>et al.</i> , 2006
	–	–	2400	75.0	–	–	7970	3040	

	–	–	610	19.1	–	–	–	–	Chen <i>et al.</i> , 2018
	–	–	1390	43.4	–	–	4310	1650	Gill <i>et al.</i> , 2013
	500	125 ¹	–	–	–	–	5660	92.3	Knights <i>et al.</i> , 2016
	–	–	580	18.1	–	–	–	–	Liang <i>et al.</i> , 2011
	–	–	1050	32.8	–	–	–	–	Rowland <i>et al.</i> , 2008
	–	–	1400	43.8	–	–	–	–	Shimizu <i>et al.</i> , 2007
	–	–	90	2.81	–	–	5800	2210	Soars <i>et al.</i> , 2001
	–	–	3800	119	–	–	–	–	Soars <i>et al.</i> , 2003
	–	–	780	24.4	–	–	–	–	Walsky <i>et al.</i> , 2012
UGT1A9	–	–	14200	444	–	–	–	–	Komura and waki 2011
MPA ^a	–	–	20500	641	–	–	–	–	Miles <i>et al.</i> 2005
	–	–	5160	161	–	–	12900	4940	Picard <i>et al.</i> 2005
UGT2B7	–	–	1120	14.5	–	–	–	–	Achour <i>et al.</i> 2018
AZT ^a	–	–	90	1.03	–	–	–	–	Chen <i>et al.</i> 2018
	5000	1000 ¹	–	–	–	–	1230	32.7	Knights <i>et al.</i> 2016
	–	–	4700	54.0	–	–	–	–	Walsky <i>et al.</i> 2012
UGT2B7	–	–	480	5.52	–	–	2000	1320	Soars <i>et al.</i> 2001
Naloxone									

^aMPA, Mycophenolic acid; AZT, Zidovudine
^bWhere activity is not specified as V_{max} or CL_{int,u}, if probe concentration is significantly above the Km value (>2-fold), activity was assumed to be at V_{max}. ¹Knights *et al.*, 2016.

Table 4. CL_{int,u} (μL/min/mg microsomal protein) and calculated CL_{int,u} per unit enzyme (μL/min/pmol enzyme) data for UGT enzymes using probe substrates, across human liver, intestine and kidney tissues

Enzyme/ identified probes	Probe		Liver		Intestine		Kidney		Study
	Conc. (μM) ^b	Km (μM) ^c	Activity	CL _{int,u}	Activity	CL _{int,u}	Activity	CL _{int,u}	
UGT1A1 <i>Ezetimibe</i>	1	–	5180	126	1160	620	495	3540	Gill <i>et al.</i> 2012
UGT1A3 <i>Telmisartan</i>	1	–	395	12.6	91.4	80.2	34.3	245	Gill <i>et al.</i> 2012
UGT1A9 <i>Propofol</i>	20	98-127 ¹	603 ^d	1.67	–	–	–	–	Bhatt <i>et al.</i> 2019
	5	–	201	1.26	–	–	1020	78.1	Gill <i>et al.</i> 2012

UGT1A9 MPA ^a	1	–	233	7.28	–	–	1370	523	Gill <i>et al.</i> 2012
	1	–	–	–	–	–	1060	405	Scotcher <i>et al.</i> 2017
UGT2B7 Naloxone	10	423- 870 ²	59.6 ^d	0.163	–	–	–	–	Bhatt <i>et al.</i> 2019
	1	–	17.4	0.200	21.4	16.0	–	–	Cubitt <i>et al.</i> 2009
	1	–	55.6	0.639	14.2	10.6	52.7	34.7	Gill <i>et al.</i> 2012
^a MPA, Mycophenolic acid ^b Probe concentration used to calculate CL _{int,u} per unit enzyme (see ‘Materials and Methods’) ^c Where activity is not specified as V _{max} or CL _{int,u} , if probe concentration was significantly below the Km value (<0.5-fold), activity was assumed to be in the intrinsic clearance range. ¹ Miners <i>et al.</i> , 2021. ² Seo <i>et al.</i> , 2014. ^d Activity after correction for fraction unbound, using calculated fu _{mic} (Gao <i>et al.</i> , 2008; Hallifax and Houston, 2006).									

Table 5. Interlaboratory differences between the literatures used for V_{max} and intrinsic clearance data, for k_{cat} and CL_{int,u} calculations, including concentrations of uridine diphosphate glucuronic acid (UDPGA), Alamethicin, MgCl₂, % of BSA.

Literature	UDPGA (mM) ^a	Alamethicin ^b	MgCl ₂ (mM) ^b	BSA (%) ^c	Buffer ^d
Achour <i>et al.</i> , 2018	5	10µg/mL	5	-	100mM Tris-HCl, pH 7.5
Al Jahdari <i>et al.</i> , 2006	3	50µg/mL	8	-	50mM Tris-HCl, pH 7.6
Benoit-Biancamano <i>et al.</i> , 2008	2	-	10	-	50mM Tris-HCl, pH 7.7
Bhatt <i>et al.</i> 2019	2.5	100µg/mL	-	0.01	100mM Phosphate, pH 7.4
Chen <i>et al.</i> 2018	-	25mg/mL	5	-	50mM Tris-HCl, pH 7.4
Cubitt <i>et al.</i> 2009	5	50µg/mL	10	-	100mM Phosphate, pH 7.1
Gill <i>et al.</i> 2012	5	50µg/mg protein	3.45	1-2 ^e	100mM Phosphate, pH 7.1
Gill <i>et al.</i> 2013	5	50µg/mL	3.45	-	100mM Phosphate, pH 7.1
Knights <i>et al.</i> , 2016	5	50µg/mg protein	4	-	100mM Phosphate, pH 7.4
Komura and Iwaki, 2011	2	50µg/mg protein	10	-	100mM Tris-HCl, pH 7.4
Liang <i>et al.</i> , 2011	5	25µg/mL	5	-	50mM Tris-HCl, pH 7.4
Miles <i>et al.</i> 2005	3	50µg/mg protein	10	-	75mM Tris-HCl, pH 7.45
Picard <i>et al.</i> 2005	2	-	10	-	100mM Tris-HCl, pH 7.4

Rowland <i>et al.</i> , 2008	5	50µg/mg protein	4	-	100mM Phosphate, pH 7.4
Scotcher <i>et al.</i> 2017	5	50µg/mg protein	3.45	1	100mM Phosphate, pH 7.4
Shimizu <i>et al.</i> , 2007	3	50µg/mL	10	-	50mM Tris-HCl, pH 7.4
Soars <i>et al.</i> 2001	5	-	10	-	100mM Tris/malate buffer, pH 7.4
Soars <i>et al.</i> , 2003	5	50µg/mL	1	-	100mM Phosphate, pH 7.1
Walsky <i>et al.</i> , 2012	5	10µg/mL	5	-	100mM Tris-HCl, pH 7.5

^aMinimum 5mM required for reliable glucuronidation activities for k_{cat} and $CL_{in,u}$ calculations (Miners *et al.*, 2021)

^bFactors influencing measured V_{max} specifically (Miners *et al.*, 2021)

^cReduces substrate K_m , impacting on measured $CL_{int,u}$ (Miners *et al.*, 2021)

^dIncreases glucuronidation activities, reflected as greater mean $CL_{int,u}$ (Badée *et al.*, 2019)

^eUGT1A1, 2% BSA; UGT1A3, 1% BSA

Figure legends

Figure 1. Comparison of abundance values for UGT enzymes in the gut and kidney, as a ratio to the liver. The liver has been used as a reference point, crossing the y-axis horizontally at 1. Plotting the y-axis in logarithmic scale (\log_{10}) demonstrates the fold difference in abundance for intestinal and renal tissues, with respect to the liver (specific fold values labelled on the graph).

Figure 2. Comparison of activity values (k_{cat}) (A) and intrinsic clearance ($CL_{int,u}$) (B) for UGT enzymes in the gut and kidney, as a ratio to the liver. The liver has been used as a reference point, crossing the y-axis horizontally at 1. Plotting the y-axis in logarithmic scale (\log_{10}) demonstrates the fold difference in abundance for intestinal and renal tissues, with respect to the liver (fold values labelled specific on the graph). Error bars are included, where there is sufficient data (i.e., ≥ 2 data sets). *MPA, Mycophenolic acid; AZT, Zidovudine

Figure 1

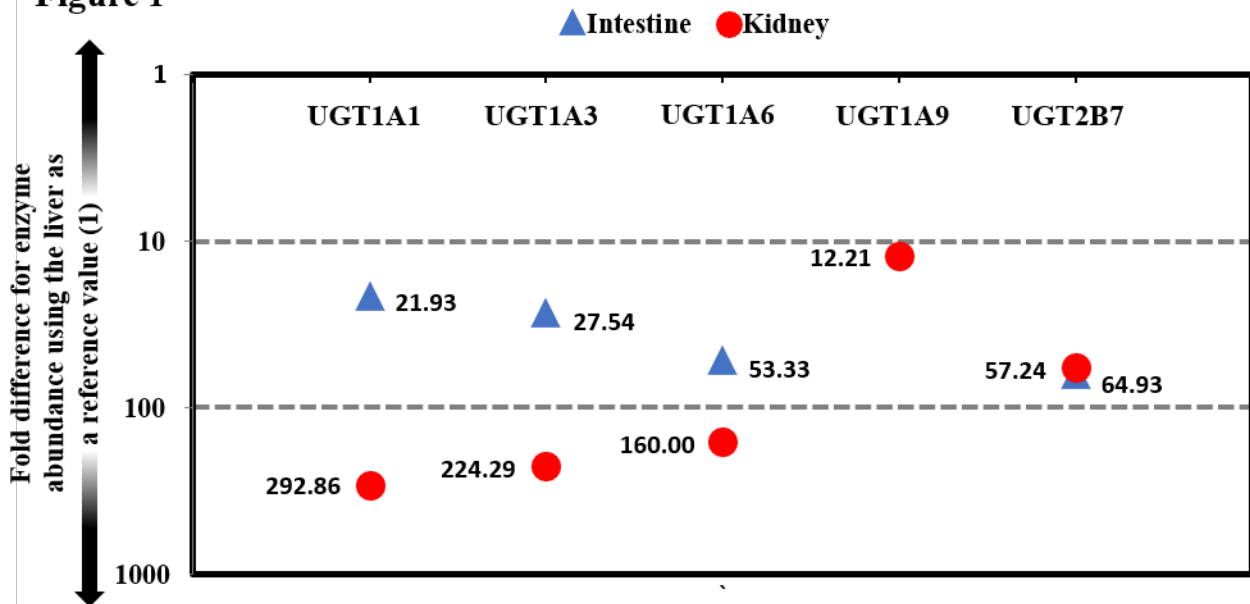


Figure 2

▲ Intestine ● Kidney

